Biochimica et Biophysica Acta, 936 (1988) 487–503
Elsevier

BBA 42878

Studies on well-coupled Photosystem I-enriched subchloroplast vesicles – characteristics and reinterpretation of single-turnover cyclic electron transfer

F.A. de Wolf, K. Krab, R.W. Visschers, J.H. de Waard and R. Kraayenhof

Biological Laboratory, Vrije Universiteit, Amsterdam (The Netherlands)

(Received 7 June 1988)

Key words: Cyclic electron transfer; Cytochrome; Ferredoxin; Plastocyanin; Membrane potential; Photosystem I

The contributions of ferredoxin, P-700, plastocyanin and the cytochromes *c*-554, and *b*-563 to single-turnover electron transfer in Photosystem (PS) I-enriched subchloroplast vesicles were deconvoluted by fitting the literature-derived spectra of these components to the observed absorption data at a series of wavelengths, according to a linear least-squares method. The obtained corresponding residuals showed that the applied component spectra were satisfactory. The deconvoluted signals of cytochromes *c*-554 and *b*-563 differed in some cases significantly from the classical dual-wavelength signals recording at 554–545 nm and 563–575 (or –572) nm, due to interference from other electron-transferring components. KCN, DNP-INT (2-iodo-6-isopropyl-3-methyl-2′,4,4′-trinitrodiphenyl ether), DBMIB (2,5-dibromo-3-methyl-6-isopropyl-*p*-benzoquinone) and antimycin A all inhibited electron transfer, although antimycin and DBMIB inhibited only after a few turnovers of the cytochrome *bf* complex. Fast flash-induced reduction of cytochrome *b*-563 exclusively reflected oxidant-induced reduction. Fast electron flow from cytochrome *c*-554 to plastocyanin and P-700 resulted in an apparent rereduction of cytochrome *c*-554 that was slower than the reduction of cytochrome *b*-563. Model simulations indicate that under highly oxidizing conditions for the Rieske FeS centre and reducing conditions for cytochrome *b*-563, the semiquinone at the Q_z site cannot only reduce cytochrome *b*-563, but can also oxidize cytochrome *b*-563 and reduce the Rieske FeS centre. The effect of 10 μM gramicidin D was evaluated in order to determine the contributions by electrochromic absorption changes around 518 nm. Gramicidin left electron transfer, monitored in the 550–600 nm range, unchanged. The gramicidin-sensitive (membrane potential-associated) signal at 518 nm differed from the signals recorded in the absence of gramicidin at 518 nm or 518–545 nm, due to spectral interference from electron-transferring components in the latter signals. KCN, DBMIB and antimycin A affected both the fast and slow components of the electrochromic signal, but did not proportionally affect the initial electron transfer from P-700 to ferredoxin (charge separation in PS I). Not only the slow (10–100 ms) component of the 518 nm absorption change, but also part of the fast (less than 1 ms) component appears to monitor electrogenic events in the cytochrome *bf* complex.

Abbreviations: Chl, chlorophyll; DAD, 2,3,5,6-tetramethyl-*p*-phenylenediamine (diaminodurene); DBMIB, 2,5-dibromo-3-methyl-6-isopropyl-*p*-benzoquinone; DMQ, 2,5-dimethyl-*p*-benzoquinone; DNP-INT, 2-iodo-6-isopropyl-3-methyl-2′,4,4′-trinitrodiphenyl ether; P-700, primary electron donor of Photosystem I; PMS, *N*′-methylphenazonium methosulphate; PS I, Photosystem I, PS II, Photosystem II.

Correspondence: F.A. de Wolf, Biologisch Laboratorium, Vrije Universiteit, de Boelelaan 1087, 1081 HV Amsterdam, The Netherlands.

Introduction

Subchloroplast vesicles, prepared by mild digitonin treatment of chloroplasts, are mainly derived from the exposed thylakoid membranes and offer a useful object for studies of cyclic electron transfer around PS I, avoiding bias due to additional electron input from PS II. Their composition [1], light-induced electric potential generation [2–5] and phosphorylating activity [6–8] has been analyzed previously. A characterization of cyclic electron flow in these vesicles has also been undertaken [3].

In line with several studies on chloroplast systems [9–14], the absorption changes of cytochrome *c*-554 (cytochrome *f*) and cytochrome *b*-563 were commonly determined from dual-wavelength experiments [3] involving registrations at 554 and 563 nm with respect to a reference wavelength. Possible interference from contributions of P-700, plastocyanin or ferredoxin [15,16] was not taken into account so far. Such interference has similarly been disregarded in studies on the behaviour of the carotenoid absorbance changes around 518 nm in PS I vesicles [2–4] and in chloroplasts [12–14,17–21]. However, the known absorption spectra of P-700 [22], ferredoxin [23], plastocyanin [24], and the cytochromes *c*-554, *b*-563 and *b*-559 [25] show substantial overlap in the wavelength range of 500–600 nm. Therefore, significant contributions of unwanted components to single- or dual-wavelength recordings of absorption changes may occur and the extent of this interference may depend on the conditions, for example in redox or inhibitor titrations. In order to improve this analysis, it is essential to determine the contributions of all involved redox components in the given wavelength range of interest. This can be done in principle if all components involved and their respective spectra are known.

Recently, a method was described to correct the absorption changes of cytochromes in photosynthetic bacteria for electrochromic absorption changes [26]. In a mixed solution of known amounts of pyridine hemochromes, a spectral deconvolution procedure for the simultaneous determination of hemochromes *a*, *b* and *c*, based on matrix inversion, appeared to be satisfactory [27]. A similar deconvolution procedure has been used to determine the light-induced absorption changes of P-700, plastocyanin and the cytochromes *c*-554 and *b*-563 in a proteoliposome system, exclusively consisting of purified and reconstituted PS I, cytochrome *bf* complex, and plastocyanin, apart from lipids and redox mediators [16]. The overall absorption changes were followed at a number of wavelengths equal to the number of deconvoluted components. However, this provides no insight into the accuracy of the deconvolution. If the absorption changes at the various wavelengths are not recorded simultaneously, such deconvolutions are not only susceptible to uncertainties about the spectral properties of the components such as they occur in the functional system, but also to temporal instabilities of the system, resulting in changes that occur in the time between the various measurements.

In more complicated systems like PS I vesicles or chloroplasts, more components are involved and consequently more wavelengths should be taken into account. In addition, the uncertainty about the number and the nature of the components involved is larger. Especially in these systems, insight into possible errors is essential. This insight is enhanced by measuring at a number of wavelengths larger than the number of deconvoluted components. In addition, this redundant spectral information may be used to increase the stability of the results obtained after deconvolution.

In the present study on PS I vesicles, we have measured the absorption changes at 8–15 different wavelengths in the 500–600 nm wavelength range and deconvoluted the contributions of the five electron transfer components that elicited the largest absorption changes in this wavelength range. Because the information on the spectral shape of the electrochromic absorption changes is not always consistent, these changes are not taken into account in the spectral deconvolution. For this reason we have performed the measurements at high gramicidin concentrations in order to prohibit these electrochromic contributions. Fortunately, it appeared that these high concentrations of gramicidin did not influence electron transfer in our system.

The deconvolution procedure appeared to be

quite satisfactory under single-turnover conditions. The results obtained by deconvolution allow a more detailed analysis of electron transfer than was previously possible [3]. In addition to the flash-induced absorption transients of cytochrome *c*-554, cytochrome *b*-563 and the membrane potential-monitoring carotenoids, those of ferredoxin, P-700 and plastocyanin could be determined as well.

Materials and Methods

The preparation of PS I vesicles and the experimental conditions were as described in [4,7,8], the temperature being 20 °C and the pH being 7.8 and 8.0 in the isolation and storage/reaction media, respectively. After preparation, the PS I vesicle batches were stored in small portions in liquid nitrogen.

Gramicidin D, DBMIB, DNP-INT, antimycin A, DAD, duroquinone, DMQ and *p*-benzoquinone were added from ethanolic solutions, the ethanol concentration in the reaction mixture never exceeding 1% (v/v). After addition, 10 min of darkness, followed by 2 min of continuous illumination and another 5 min of darkness were applied to reach full effectivity of these agents. The final gramicidin concentration was always 10 μM. Two times higher or lower concentrations had the same effect. KCN inhibition was effected by preincubating the vesicles during 60 min in the dark at 0 °C, in the absence of ferredoxin and NADPH and at a final concentration of 50 mM KCN. After this incubation, ferredoxin and NADPH were added to the reaction mixture, as normally.

DBMIB and DNP-INT were kindly donated by Prof. A. Trebst (Ruhr-Universität, Bochum, F.R.G.). Gramicidin D and antimycin A were purchased from Boehringer (Mannheim, F.R.G.); DAD was purchased from Aldrich (Beerse, Belgium), duroquinone from BDH (Poole, U.K.), DMQ from Eastman/Kodak (Rochester, NY, U.S.A.), *p*-benzoquinone from Fluka (Buchs, Switzerland) and PMS from Sigma (St. Louis, MO, U.S.A.). All other chemicals were purchased from Merck (Darmstadt, F.R.G.).

The single-turnover experiments were carried out in a previously described, laboratory-built kinetic spectrophotometer [2,4,28,29]. Saturating actinic Xe flashes (tail-depressed, 5 μs at half maximal amplitude) were fired at 0.1 Hz. The absorption transients following 50–100 flashes were averaged.

In the course of the experiment, several times between the measurements at the various wavelengths (and in any case at the end of each experiment), a set of transients was again recorded at the initially used wavelength in order to check that no instabilities or ageing had occurred during the experiment. In general, the presently used samples were stable for about 3 h. Thereafter, the experiment was continued with a freshly thawed portion of vesicles and it was checked at one or two wavelengths that these vesicles behaved in exactly the same way as the previous portion of vesicles. The results obtained with different portions of the same PS I vesicle batch were usually equal. If not, they were discarded.

The spectral information about the various electron-transferring components involved in the present PS I vesicle system was derived from the following literature for: ferredoxin [23,30–32], P-700 [22], plastocyanin [24] and cytochromes *c*-554 and *b*-563 [25,33]. The actual data applied in the deconvolutions are shown in Table I.

Only the contributions of ferredoxin, P-700, plastocyanin and the cytochromes *c*-554 and *b*-563 were taken into account under our experimental conditions. This appeared to be satisfactory. From Fig. 4 of Ref. 3 it appears that in the presence of the $NADP^+$/NADPH redox-poising system there is also a small contribution by cytochrome *b*-559. Apparently, there was no contribution of cytochrome *b*-559 under our conditions (no $NADP^+$ present), but it cannot be excluded that the deconvoluted cytochrome *b*-563 signal can occasionally contain a contribution by cytochrome *b*-559. If only cytochrome *b*-563 was taken into account, very satisfactory residuals (see below) were obtained, also around 559 nm.

In the present experiments, the recorded absorption transients consisted of 512 data points, sampled at about 400 μs intervals. The deconvolutions were carried out with a computer according to the following procedure. Using the transients obtained at m different wavelengths (m in the range of 8–15), an $m \times 512$ array was composed.

This array, designated here as S, accordingly comprised 512 spectra. From the normalized extinction coefficients shown in Table I, a selection was made that corresponded to the five components to be deconvoluted and the m wavelengths used, in order to create an $m \times 5$ array (E).

First, the so-called pseudo-inverse of E was calculated, using the Gauss-Jordan method and (to minimize the computational error) 'partial pivoting' [34]:

$$(E^{T} \cdot E)^{-1} \cdot E^{T}$$

The contribution of the five components to the overall absorption changes (at any of the 512 points in time) was then calculated as a 5×512 array (C):

$$C = (E^{T} \cdot E)^{-1} \cdot E^{T} \cdot S$$

Thus, C comprises the absorption transients of the five deconvoluted components at their peak wavelengths (525 nm for P-700 and 500 nm for ferredoxin, see Table I), calculated according to a linear least-squares method.

In principle, measurements at only five different wavelengths ($m = 5$) would suffice to calculate C. (The pseudo-inverse of E would then become equal to E.) The redundant information obtained by measuring at more than five wavelengths increases the stability of the solution and allows an error analysis. Using the literature-derived spectra of the individual components (Table I, E), each weighted according to its individual contribution as defined by C, an overall spectrum (fitted spectrum) was calculated at any of the 512 points in time:

$$F = E \cdot C$$

Thus, the $m \times 512$ array F comprises 512 spectra, or m absorption transients, representing the fitted transient at the m wavelengths used. The residuals can then be calculated as the difference between the originally recorded transients and the fitted transients:

$$R = S - F$$

where R is also an $m \times 512$ aray and comprises the residuals (absorption transients) at m wavelengths. These residuals cannot be described in terms of the spectral components as they were assumed to be (Table I), since the spectral 'spaces' defined by the columns of R and E are orthogonal. The residuals reflect errors in the fit such as caused by neglected components, light scattering, etc.

Results

The electrochromic signals – the effect of gramicidin

In the absence of NADPH, but in the presence of ferredoxin, no flash-induced absorption changes were observed at all in the 480–600 nm range (not shown). Electron transfer is not seen under those conditions, due to full oxidation of all redox carriers involved. After reduction of the system by 500 μM NADPH, flash-induced absorption transients were observed (Fig. 1), monitoring electron transfer and membrane potential formation. 10 μM gramicidin seriously affected the absorption changes in the 480–550 nm range, but was without any effect in the 550–600 nm range. Fig. 1 shows these effects at some important wavelengths in these ranges. Apparently, gramicidin does not significantly affect cyclic electron transfer itself. The gramicidin-sensitive part of the transients (right column of traces in Fig. 1) seems to reflect the electrochromic absorption band shift around 480–520 nm. The fast (0–3 ms) component which is seen around 518 nm in the absence of gramicidin is abolished very rapidly, so as to reveal even a fast absorption decrease (Fig. 1). It seems that the full extent of the electrochromic absorption changes, detectable under our conditions (time resolution, 400 μs), was cancelled by gramicidin, since transient absorption changes (decaying within less than a few ms) were not observed (neither in the absence nor in the presence of gramicidin).

In the gramicidin-sensitive electrochromic signal at 520 nm the 'slow' component (peaking at 40–50 ms)is not as slow as in the original signal in the absence of gramicidin (peaking at 70–100 ms). Fig. 1 shows that at 520 nm, there is also an important contribution of gramicidin-resistent (non-electrochromic) absorption changes. The non-electrochromic signals vary with the wavelength (Fig. 1) and the conditions (see below).

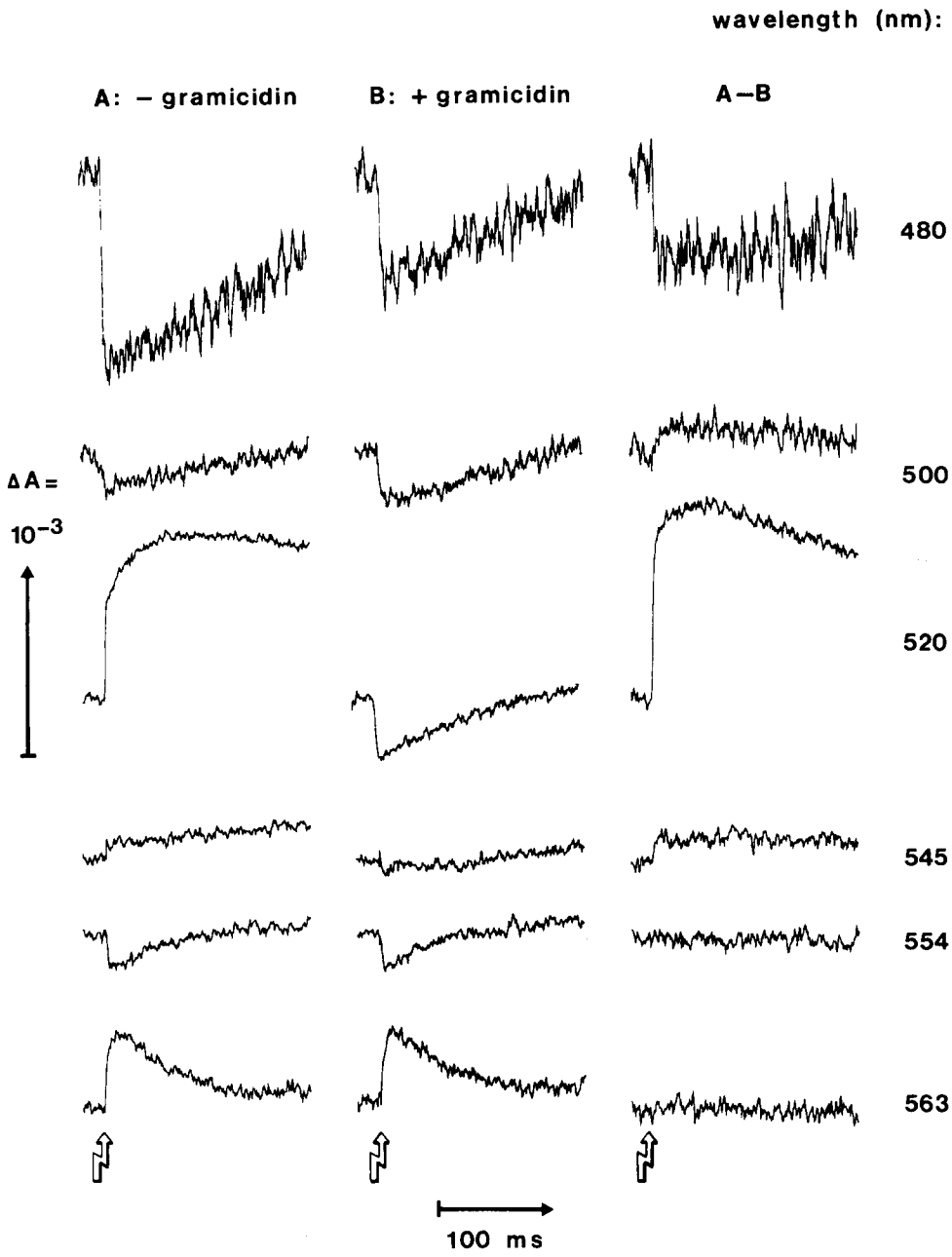

Fig. 1. Flash-induced absorption transients in the absence and presence of 10 μM gramicidin D. The reaction mixture contained 250 mM sorbitol, 20 mM NaCl, 20 mM KCl, 5 mM $MgCl_2$, 2.5 mM KH_2PO_4, 1 mM Tes/KOH buffer, 500 μM NADPH, 5 μM ferredoxin and about 100 μM O_2 at pH 7.8 and 20 °C. Vesicles were added to 50 μg Chl·ml^{-1}. The right column shows the gramicidin-sensitive parts of the of the original transients. The open arrows indicate the moment of flashing.

Therefore, the original transients (in the absence of gramicidin) recorded at 518 or 518–545 nm [2–5,9,12–14] do not exclusively reflect electrochromic effects. When the refer to "electrochromic signal" below, the gramicidin-sensitive absorption change at 518 nm is meant.

The spectral components detectable in the presence of gramicidin

Since 10 μM gramicidin did not affect electron transfer (judged from the lack of effect in the 550–600 nm range), we chose to measure the absorption changes of the electron-transferring components in the presence of gramicidin. This prevented interfering electrochromic absorption changes. Fig. 2 shows the deconvoluted absorption changes of ferredoxin, P-700, plastocyanin and the cytochromes *c*-554 and *b*-563 at high ambient redox potential (about 485 mV) established by potassium ferricyanide and ferrocyanide in the presence of redox mediators (see legend to Fig. 2). Plastocyanin and the cytochromes did not contribute to the flash-induced absorption changes, since they were already oxidized before the flash. Ferredoxin reduction was not detected, possibly because the reoxidation rate was too high in the presence of ferricyanide (and redox mediators). Also in the absence of ferricyanide, under the conditions of Fig. 1, but with duroquinone present, ferredoxin reduction was not observed (not shown). Thus, it is possible that duroquinone elicited fast ferredoxin oxidation, or drew away electrons between P-700 and ferredoxin. The only significant redox change observed is that of P-700. Apparently, no complete rereduction of P-700 occurred in the course of 200 ms, showing that electron flow through the artificial redox mediator system to P-700 was slow. However, the presence of a P-700 signal in the averaged traces shows that at least some P-700 rereduction occurred within the 10 s interval between subsequent flashes: otherwise the individual flash-induced signals would have been abolished already after the first few flashes and the average would have become virtually zero (this is not observed; the average of 100 flashes is shown). A flash interval of double duration (20 s) did not change the results (not shown), indicating that in the presence of the applied redox mediators, the 10 s flash interval

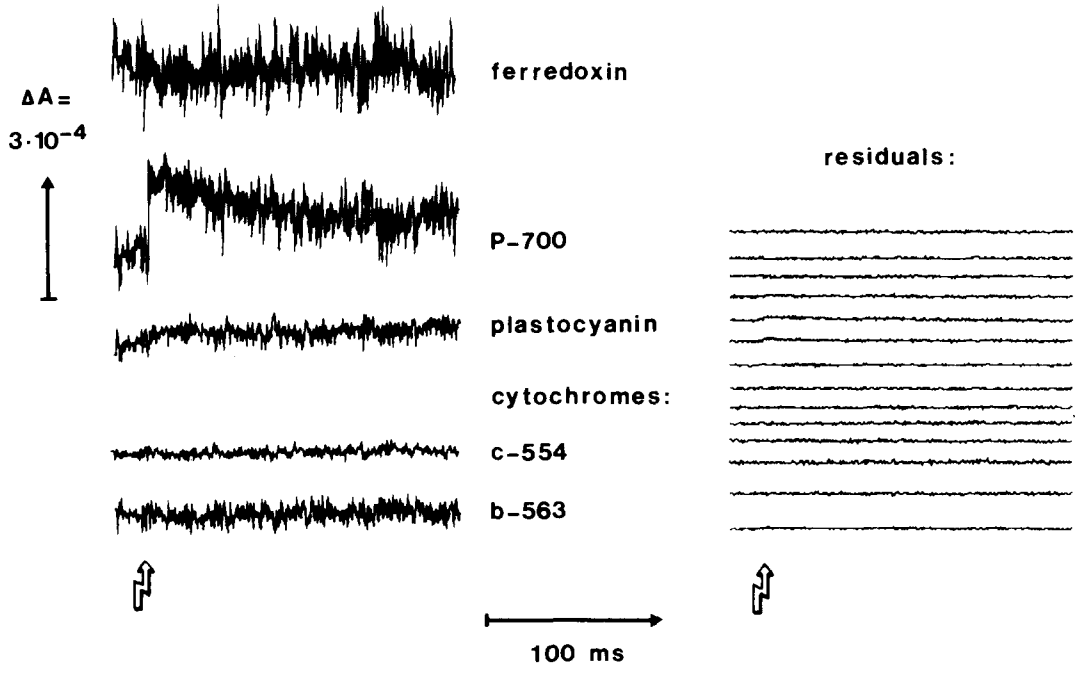

Fig. 2. The deconvoluted contributions of ferredoxin, P-700, plastocyanin and the cytochromes *c*-554 and *b*-563 under oxidizing conditions and in the presence of 10 μM gramicidin D. The contributions are shown as absorption changes at 500, 525, 590, 554 and 563 nm for ferredoxin, P-700, plastocyanin and the cytochromes *c*-554 and *b*-563, respectively. On the right (from top to bottom) the residuals at 515, 520, 525, 537, 540, 545, 550, 554, 559, 563, 566, 570, 575 and 590 nm are shown. Open arrows indicate the moment of flashing. Potassium ferricyanide (10.8 mM), potassium ferrocyanide (1.2 mM), duroquinol (10 μM), DMQ (10 μM), PBQ (10 μM) and PMS (1 μM) were present; NADPH was absent. Further conditions as in Fig. 1.

TABLE I

NORMALIZED EXTINCTION COEFFICIENTS USED IN THE SPECTRAL DECONVOLUTIONS

The reduced-minus-oxidized coefficients of each component were normalized to the largest coefficient occurring in the 500–600 nm wavelength range (values in $mM^{-1} \cdot cm^{-1}$): 3.6 (ferredoxin at 500 nm), 5.8 (P-700 at 525 nm), 4.7 (plastocyanin at 590 nm), 20.0 (cytochrome *c*-554 at 554 nm), 14.5 (cytochromes *b*-563 and *b*-559 at 563 and 559 nm, respectively).

Wavelength (nm)	Extinction coefficient of					
	ferredoxin	P-700	plastocyanin	cytochrome		
				c-554	*b*-559	*b*-563
500	−1.000	−1.146	0.148	−0.284	−0.158	−0.197
515	−0.817	−0.802	−0.216	−0.065	−0.032	0.000
520	−0.750	−0.926	−0.245	0.073	0.027	0.141
525	−0.706	−1.000	−0.269	0.104	0.075	0.274
530	−0.649	−0.990	−0.312	−0.028	0.153	0.380
537	−0.590	−0.831	−0.345	−0.143	0.036	0.521
540	−0.565	−0.767	−0.404	−0.113	−0.048	0.464
545	−0.522	−0.686	−0.463	0.049	−0.067	0.354
550	−0.500	−0.672	−0.515	0.707	0.110	0.303
554	−0.456	−0.637	−0.588	1.000	0.463	0.393
559	−0.413	−0.569	−0.651	0.089	1.000	0.745
560	−0.406	−0.558	−0.660	−0.063	0.959	0.855
562	−0.392	−0.507	−0.689	−0.197	0.863	0.955
563	−0.380	−0.497	−0.702	−0.217	0.792	1.000
566	−0.356	−0.411	−0.748	−0.252	0.370	0.825
570	−0.321	−0.233	−0.814	−0.226	0.000	0.259
572	−0.305	−0.148	−0.874	−0.222	−0.134	0.039
575	−0.281	−0.021	−0.905	−0.195	−0.219	−0.099
590	−0.268	0.411	−1.000	−0.085	−0.137	−0.103

was enough for complete relaxiation of P-700 to the equilibrium reduction level.

The residuals shown in Fig. 2 indicate that the P-700 spectrum applied in the deconvolution (Table I) fitted well to the observed absorption changes and that it corresponded indeed to the spectrum of the P-700 functioning in these vesicles. Also, the quality of the fit indicates that no significant electrochromic absorption changes remained in the presence of gramicidin, since these could not have been fitted precisely with the spectrum of P-700 (see also the residuals in Fig. 3).

In Fig. 2, i.e., at about 485 mV, the amount of flash-oxidized P-700 was about 30 to 60% of the amount in control experiments. The flashes were saturating and thus elicited full oxidation of P-700. Assuming full reduction before the flash in control experiments, our data would correspond to a midpoint potential of about 465 to 500 mV for P-700. This is indeed in the range of potentials determined by others [35,36]. A more detailed study of the redox-potential-dependent behaviour of the signals is under investigation and will be published later.

For a further test of the deconvolution method, KCN was used in an experiment where the system was redox-poised by 500 μM NADPH and 100 μM oxygen (standard conditions). Fig. 3 shows that now there is also a contribution of ferredoxin. In agreement with earlier observations [36,37], KCN inhibits plastocyanin effectively, since rereduction of P-700 did not occur in the course of 200 ms and a contribution from plastocyanin and the cytochromes (compare with Fig. 4) was absent. In comparison with the control situation (see below, Fig. 4), the extent of the flash-induced P-700 oxidation in Fig. 3 indicates that 30 to 60% rereduction of P-700 did occur in the course of the flash interval (10 s). From the residuals shown in Fig. 3, it appears that not only the spectrum of P-700 (Table I) was satisfactory (this followed from Fig. 2), but also the spectrum of ferredoxin

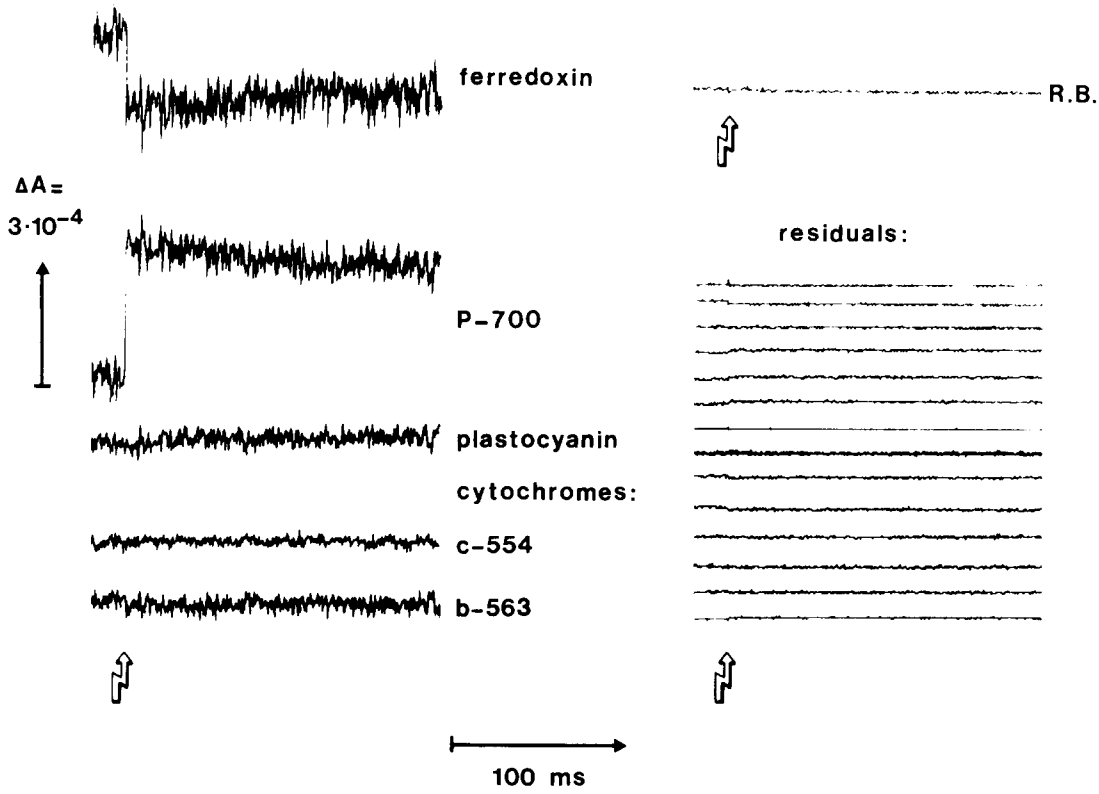

Fig. 3. Deconvoluted absorption transients in the presence of 50 mM KCN and 10 μM gramicidin D. Shown are the five components as indicated in the figure together with the residuals at (from top to bottom) 515, 520, 525, 537, 540, 545, 554, 559, 562, 563, 566, 570, 575 and 590 nm. The trace indicated by R.B. is the net reduction balance (obtained by dividing each deconvoluted signal by its proper millimolar extinction coefficient and by making a linear combination of the resulting signals such that net reduction corresponds to an upward deflection).

(Table I). Moreover, the flash-induced millimolar amounts of P-700 oxidized and ferredoxin reduced matched precisely. This is shown by the net reduction balance of the system (Fig. 3), calculated as the sum of the flash-induced millimolar reduction of ferredoxin, P-700, plastocyanin, and the cytochromes *c*-554 and *b*-563, using the millimolar extinction coefficients that are shown in the legend of Table I. The flash-induced absorption changes of ferredoxin (Fig. 3, see also Figs. 4 and 5) are maximal around 420 and will cause a large flash-induced absorption decrease in the 'carotenoid area' around 480–520 nm. This can be seen in Fig. 1 (middle column of traces).

Cyclic electron transfer involving the cytochromes

In the presence of KCN fast electron transfer through cytochrome *b*-563 is totally abolished (compare Fig. 3 with Fig. 4). Ferredoxin is rapidly reduced, but ferredoxin reoxidation is very slow. Apparently, the previously proposed [3] fast ferredoxin-dependent reduction of cytochrome *b*-563 (c.f. Refs. 38 and 39) does not occur upon flashing, in agreement with Ref. 40. A slow reaction between ferredoxin and cytochrome *b*-563 has been demonstrated with the isolated complexes [41], but it is not likely that such a reaction occurs in the PS I vesicles (see Discussion). Fig. 4 shows the behaviour of the deconvoluted electron transfer components in uninhibited PS I vesicles. Now P-700 is completely rereduced within 20–25 ms and ferredoxin is slowly oxidized. Also, plastocyanin and the cytochromes now clearly participate in electron transfer.

After flash-induced oxidation, plastocyanin was rereduced at a somewhat slower rate than P-700.

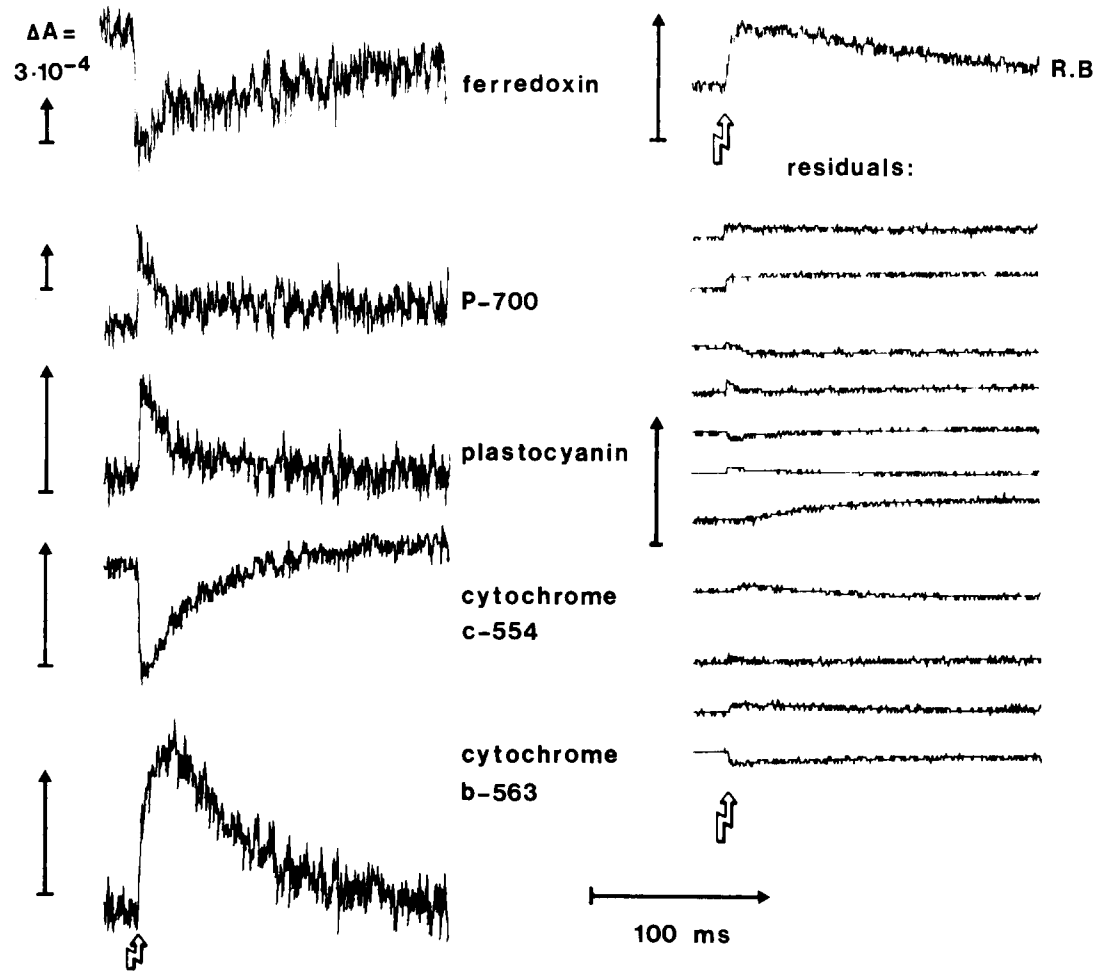

Fig. 4. Deconvoluted absorption transients of the five indicated electron-transferring components in the presence of 10 μM gramicidin D. Residuals at (from top to bottom) 515, 520, 537, 540, 545, 554, 559, 563, 570, 575 and 590 nm and reduction balance (R.B.) are shown on the right. All vertical calibration arrows correspond to $\Delta A = 3 \cdot 10^{-4}$.

Rereduction of cytochrome *c*-554 was in turn slower than that of plastocyanin. This is in agreement with the relative midpoint potentials of these components if it is assumed that electron transfer between these components is so fast that they 'equilibrate'. Cytochrome *b*-563 was rapidly reduced with apparent multiphasic kinetics. The reduction was faster than the net rereduction of cytochrome *c*-554 and much faster than the apparent reoxidation of ferredoxin.

The reoxidation of cytochrome *b*-563 was comparatively slow, but not as slow as the reoxidation of ferredoxin. This is apparently not in agreement with a (ferredoxin-dependent) reductant-induced oxidation mechanism proposed for cytochrome *b*-563 [42] (but see Discussion). The net reduction balance of the system (see above) monitors input of electrons, possibly from plastoquinone and the Rieske FeS centre, which are not directly detected (see below).

Due to the involvement of five components (Fig. 4) instead of only one or two, the spectral situation in control vesicles is much more complex than the situation shown in Figs. 2 and 3. As a consequence, the deconvolution is more susceptible to errors. This is reflected by the residuals in Fig. 4. Possibly, there is some spectral interference by quinone radicals, of which we don't know the

precise spectrum. In general, however, the deconvolution seems still satisfactory. In the experiments shown in Fig. 5, the fit was comparatively better.

The large absorption changes due to ferredoxin, P-700 and plastocyanin (Figs. 2–4), compared to those of the cytochromes, clearly show that without a proper spectral deconvolution, no reliable information on cytochrome behaviour can be obtained in this system.

As shown in Ref. 1, the amount of P-700 present in these vesicles exceeds the amount of plastocyanin and, to a larger extent, the amount of cytochromes. From the experiment shown in Fig. 4, it appears that the apparent molar ratios of P-700, ferredoxin, plastocyanin, cytochrome *c*-554 and cytochrome *b*-563 turning over were in the proportion of 1 : 2 : 0.4 : 0.1 : 0.2.

Oxidation of half the amount of P-700 necessary to explain the extent of the fast reduction of ferredoxin was not detected on this time scale (400–800 μs). This could be partly explained by the observed very rapid oxidation of plastocyanin and cytochrome *c*-554. When it is assumed that the Rieske FeS center is oxidized in parallel to cytochrome *c*-554, this can explain 60% of the missing electron equivalents. The remaining 40% could then be derived from fast electron input from plastoquinol. Since the fast flash-induced reduction of cytochrome *b*-563 was sensitive to KCN (cf. Figs. 3 and 4), reduction could not be by ferredoxin, but must be the result of oxidant-induced reduction [43–46] via the Q_z site. According to the considerations above, the electron flow from the plastoquinol pool to P-700 would be sufficiently fast to account for such a fast reduction of cytochrome *b*-563 and is in agreement with Ref. 16. The observed kinetics imply that cytochrome *c*-554 must have turned over 4–5 times within the first milliseconds after the flash. The fast input of electrons from plastoquinol to the oxidizing side of PS I and to cytochrome *b*-563 is immediately apparent from the net reduction balance (Fig. 4). Under anaerobic, reduced conditions for ferredoxin (in the presence of dithionite and glucose with glucose oxidase as oxygen scavenger) flash-induced reduction of cytochrome *b*-563 could still be observed. (Not shown; only in the presence of appropriate redox-mediators, cytochrome *b*-563 was fully reduced by dithionite and a net oxidation of cytochrome *b*-563 was induced by flashes at low flash frequency.)

The effect of electron-transfer inhibitors

The left and middle parts of Fig. 5 show that the Q_z site-inhibitors DNP-INT and DBMIB [43–48] inhibited the rereduction of cytochrome *c*-554, plastocyanin and P-700. However, DBMIB did not fully inhibit cytochrome *b*-563 reduction and cytochrome *c*-554 rereduction. The reduction balance shown in Fig. 5 (left) shows that during the first few ms after the flash, DBMIB does not prevent net input of electrons (as KCN does, cf. Fig. 3), but that inhibition occurred only after this initial phase. Note that, due to the excess of P-700 present, a single turnover of the photosystem results in several turnovers of the cytochrome *bf* complex. Like DBMIB, antimycin A inhibited electron flow only after a few turnovers of the cytochrome *bf* complex (Fig. 5), although the kinetics of the electron input were different from those obtained with DBMIB (see reduction balances). The flash-induced reduction of cytochrome *b*-563 in the presence of antimycin was smaller than in the presence of DBMIB (Fig. 5). The effect of antimycin A resembles the effect observed in an earlier study [49]. The interpretation of the effects of DBMIB and antimycin will be discussed below.

Flash-induced membrane potential generation

Fig. 6 shows the flash-induced electrochromic, gramicidin-sensitive absorption transients at 518 nm in the presence of the inhibitors KCN, DBMIB and antimycin A. These inhibitors all affected both the slow and the fast component of the electrochromic signal (peaking around 40–50 ms and within a few ms respectively, cf. Refs. 2 and 9). In chloroplasts, antimycin and DBMIB are generally found to inhibit only the slow phase of the electrochromic signal [2,9,12,13,18,19]. In few cases, also an effect of antimycin on the fast phase was noted [17,20]. We observed the effect of the inhibitors on the fast (0–3 ms) phase only when the electrochromic signal was obtained after the correction as in Fig. 1 (see also Fig. 7). The slow (40–50 ms) component seems to be affected more or less in proportion to the fast component (Fig.

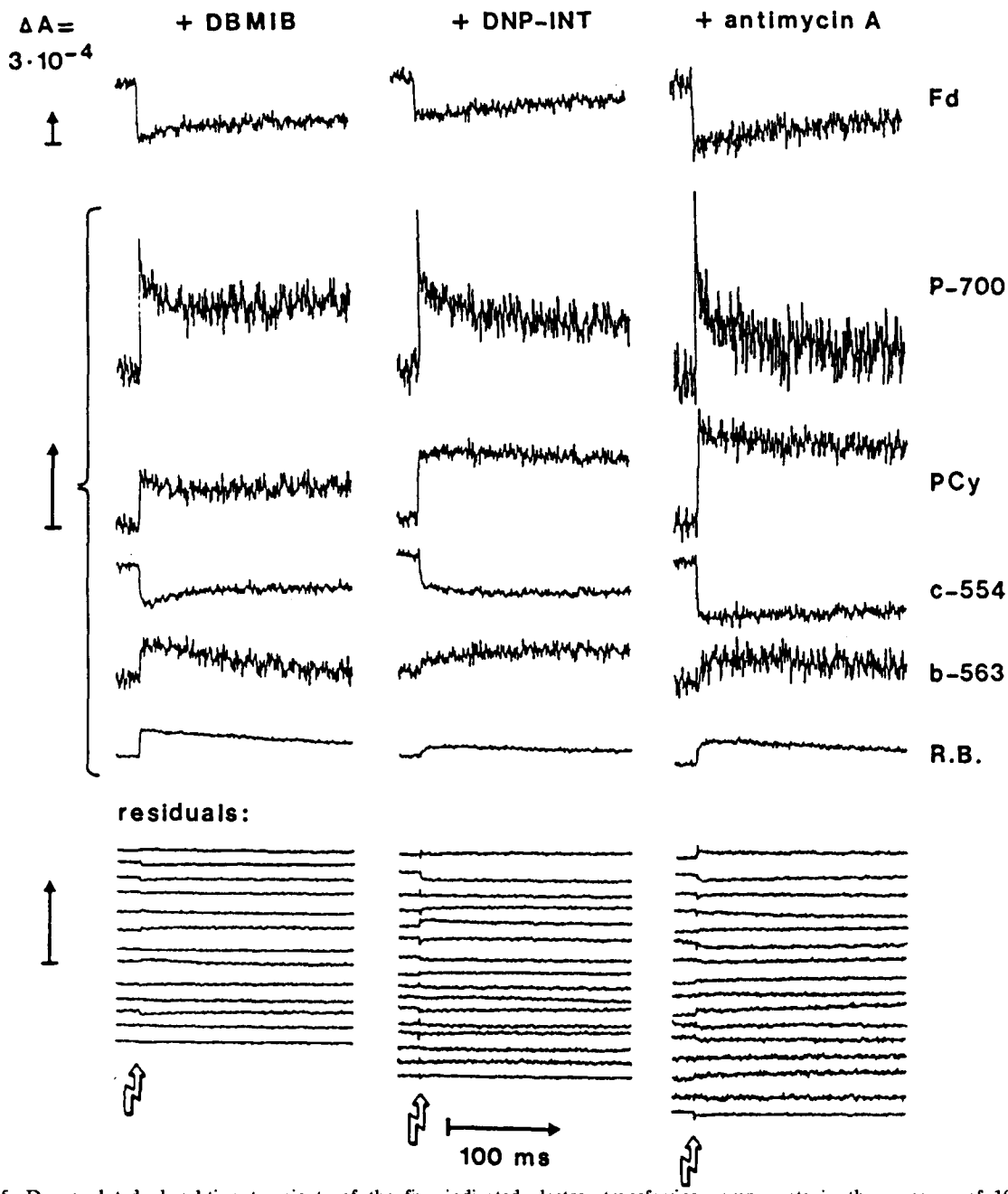

Fig. 5. Deconvoluted absorbtion transients of the five indicated electron-transferring components in the presence of 10 μM gramicidin, and of 5 μM DBMIB, 10 μM DNP-INT, or 10 μM antimycin A, as indicated. Fd = ferredoxin, PCy = plastocyanin, *c*-554 and *b*-563 = cytochrome *c*-554 and *b*-563. Residuals DBMIB experiment (left, from top to bottom) at 515, 520, 525, 537, 540, 554, 559, 562, 563, 566, 570 and 590 nm; residuals DNP-INT and antimycin A experiments (middle and right, from top to bottom) at 515, 520, 525, 537, 540, 545, 550, 554, 559, 562, 563, 566, 570, 572, 575, and 590 nm. R.B., reduction balances. The vertical calibration arrows all correspond to $\Delta A = 3 \cdot 10^{-4}$.

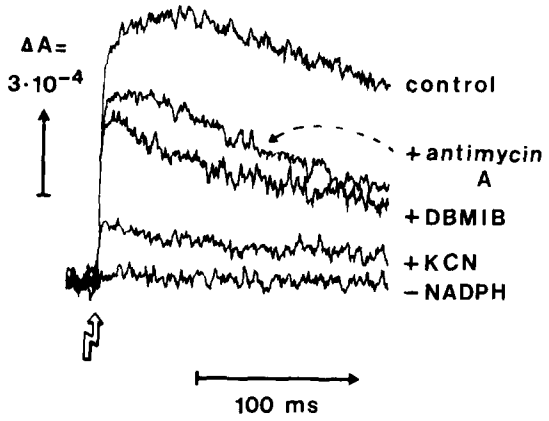

Fig. 6. The gramicidin-sensitive (electrochromic) part of the absorption transients at 518 nm in the absence and presence of the indicated inhibitors. The inhibitor concentrations were as in Figs. 3 and 5. As indicated, NADPH was absent in one experiment (lowest trace).

6). The effect of the inhibitors suggests that under these conditions only part of the fast electrochromic signal is associated with charge separation by PS I. In the absence of NADPH (bottom trace), no electron transfer occurred and accordingly no flash-induced membrane potential is generated.

Comparison of the deconvoluted signals with those directly obtained by the classical dual-wavelength method

Fig. 7 shows the flash-induced absorption changes at 518–545 nm or just at 518 nm (left) and at 554–545 nm, 563–575 or 563–572 nm (middle and right, respectively), as they occurred under similar conditions as in Figs. 1–5. The absorption changes at these wavelengths (pairs) are frequently taken to be those of the carotenoids

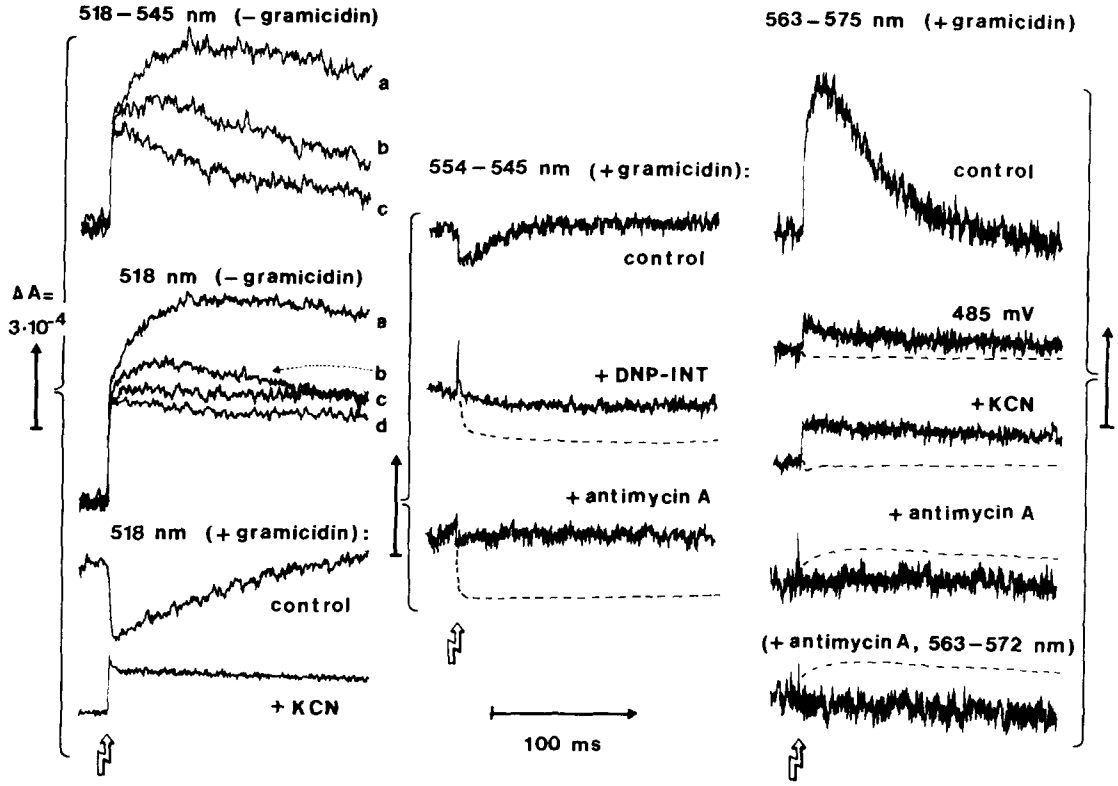

Fig. 7. Absorption transients recorded at the indicated wavelengths or wavelength pairs and in the absence and presence of the indicated inhibitors. The inhibitor concentrations were as in Figs. 3 and 5. The trace marked [485 mV' was obtained under the conditions of Fig. 2. For comparison, the deconvoluted signals (derived from Figs 2–5) of cytochrome *c*-554 (middle column) and *b*-563 (right column) are shown as dashed lines. For the traces obtained at 518 or 518–545 nm (left): a, control; b, +*DBMIB*; c, + antimycin A; d, + KCN. The vertical calibration arrows all correspond to $\Delta A = 3 \cdot 10^{-4}$.

(in response to changes of the membrane potential), cytochrome *c*-554 and cytochrome *b*-563, respectively [10–14,16–21]. It appears from Fig. 7 that under several conditions, this classical type of recording differs significantly from the deconvoluted signals shown in Figs. 3–5 and from the gramicidin-sensitive signals in Fig. 6, due to interference by absorption changes caused by P-700, ferredoxin and plastocyanin. For instance, in the absence of gramicidin (Fig. 7, left), electron-transfer inhibitors did not affect the fast component of the absorption signal at 518 nm, in contrast to what happens to the electrochromic signal in Fig. 6 (data both derived from the same experiment).

Discussion

The electrochromic signals

The data in Figs. 1, 6 and 7 clearly show that the signals observed around 518 nm or at 518–545 nm do not exclusively reflect changes of membrane potential, but contain an important contribution of electron-transferring components. The residuals shown in Figs. 2–5 show that all gramicidin-insensitive absorption changes between 500 and 600 nm are the result of redox changes in the contributing components.

The agreement of our results using classical methods (Fig. 7) with those previously obtained in PS I vesicles [2,3] and chloroplasts [9,12–14,17–21] indicates that the present results are not exceptional. We feel that previous interpretations concerning the 518 nm and other transients in PS I vesicles and chloroplasts should be reconsidered on the basis of the more accurate deconvolution data.

The effects of electron-transfer inhibitors in Fig. 6 show that electron transfer through the *b* cytochromes is not exclusively associated with the slow (40–50 ms) component of the gramicidin-sensitive signal. Also the fast (0–3 ms) component of this electrochromic signal seems to monitor in part electrogenic electron transfer from the Q_z to the Q_c-site. This implies that correlation of the slow phase with electrogenic electron transfer through the *b* cytochromes is subject to criticism. It is even conceivable that the slow component may not monitor transmembrane (electrogenic) electron transfer at all, but only an electrogenic process that results from it, such as proton movements from the external aqueous phase to the plastoquinol anion following plastoquinone reduction by cytochrome *b*-563. (Note that the slow phase is apparently affected in proportion to the fast phase, in the presence of the various inhibitors, see Fig. 6.)

Deconvolution of electron-transferring components

Spectral deconvolution not only allows to determine the simultaneous contribution of several important electron-transfer components, but is essential for a proper interpretation of the absorption transients. This is illustrated by the following example. In a previous study on PS I vesicles [3], reoxidation of cytochrome *b*-563 (monitored at 563–572 nm) and rereduction of cytochrome *c*-554 (detected at 554–545 nm) were inhibited under mild oxidizing conditions. The inhibition of cytochrome *c*-554 rereduction in Ref. 3 probably also affected P-700 rereduction. Consequently, the signal obtained at 563–572 nm may have contained a large contribution of P-700 (cf. Fig. 5), the more so as there is an excess of P-700 relative to cytochrome *c*-554 in the PS I vesicles. Thus, we can now deduce that in Ref. 3 cytochrome *b*-563 reoxidation was probably not impaired. Rather, reduction of cytochrome *b*-563 was impaired together with rereduction of cytochrome *c*-554. At 563–572 nm the main changes could have been caused by P-700, rather than cytochrome *b*-563.

Modelling the electron-transfer mechanism

In an attempt to explain our data in a more quantitative way, we carried out computer simulations based on the simple reaction scheme in Fig. 8. We varied the relative amounts of the various components and the second-order rate constants and checked the effect elicited by inhibition of quinol oxidation (at the Q_z site). However, we were not able to simulate the experimental data of Figs. 2–5 this way. The main problem was that the kinetics during turnover and the amounts of components turning over could not be fitted correctly at the same time.

A realistic excess of P-700 would tend to keep cytochrome *c*-554, plastocyanin and P-700 oxidized and cytochrome *b*-563 reduced for a

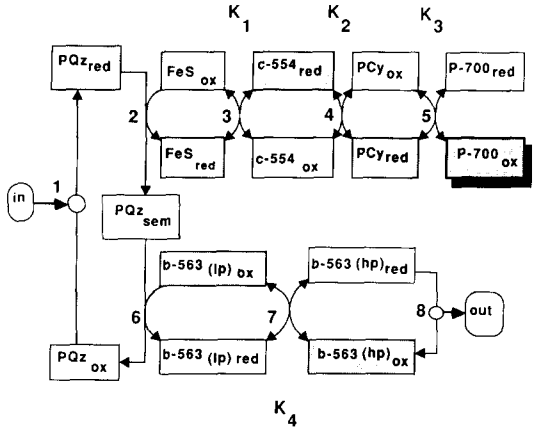

Fig. 8. The basic reaction scheme used in the computer simulations. The abbreviations are: *c*-554, *b*-563 = cytochrome *c*-554 and *b*-563, respectively. FeS = Rieske FeS centre, hp = high (midpoint) potential, lp = low potential, ox = oxidized, PCy = plastocyanin, PQ_z = bound plastoquinone at the Q_z-site, red = reduced, sem = semiquinone. Reactions 3, 4, 5, 7 are second-order equilibrium reactions. In accordance with the literature-derived midpoint potentials of the various components [43,50], the equilibrium constants were assigned the following values: $K_1 = 5.5$, $K_2 = 4.2$, $K_3 = 30$, $K_4 = 88$. The rate of reaction 1 was proportional to the amount of $PQ_{z_{ox}}$, that of reaction 8 to the amount of *b*-563 $(hp)_{red}$.

while, unless the reoxidation rate of cytochrome *b*-563 and the reduction rate of the Rieske FeS centre were drastically increased. However, the latter would result in much faster apparent (overall) rates of rereduction of cytochrome *c*-554 and reoxidation of cytochrome *b*-563 than where observed in Fig. 4.

The quality of the simulations was not improved by assuming (1) partial reduction of the quinones involved; (2) equilibrium reactions at the reaction steps 1, 2 and 6 in Fig. 8; or (3) a reoxidation rate of cytochrome *b*-563 that was not only dependent on the amount of reduced cytochrome *b*-563 (hp), but also on the amounts of quinone and reduced cytochrome *b*-563 (lp). Thus, as a modification of the model in Fig. 8, we had to assume that the reduction of the Rieske FeS centre, the reoxidation of cytochrome *b*-563 and the dissipation of the semiquinone at the Q_z-site were all intrinsically much faster during the first few milliseconds after the flash than after about 25 ms.

A sufficient increase of the rate of cytochrome *b*-563 reoxidation during the first few ms after the flash, in combination with a fast flash-induced reduction (as observed in Fig. 4), was only obtained by assuming that the semiquinone created at the Q_z-site could not only reduce cytochrome *b*-563 via the Z_z-site, but also oxidize cytochrome *b*-563 via the Q_c-site, in agreement with [16,51] (see also Refs. 52 and 53 for a similar mechanism in the mitochondrial bc_1 complex).

In order to increase the initial rereduction rate of the Rieske FeS centre, it was necessary to assume in addition that the semiquinone at the Q_z-site could elicit a second reduction of the Rieske FeS centre, in agreement with [54,55]. As noticed, this effect of semiquinone should only occur during the first few milliseconds after the flash; otherwise, complete rereduction of plastocyanin and especially of cytochrome *c*-554 would occur in a much shorter time than was observed.

The physiological background of such a kinetic effect may be that conformational changes or charge rearrangements in the cytochrome *bf* complex play a role, influencing the functioning of the Q_z-site. Without necessarily implying a mechanistic explanation of the results, a reasonable fit was obtained by (abstractly) assuming that the quinol-, and semiquinone-dependent reduction of the Rieske FeS centre (not the oxidation of cytochrome *b*-563) was proportional to the fifth power of the amount of oxidized cytochrome *c*-554 (Fig. 9, cf. Fig. 4). It is not unthinkable that the redox state or the electrical charge of cytochrome *c*-554 would trigger conformational changes that influence the Q_z-site. Alternatively, the electrical charge in the cytochrome *c*-554/Rieske FeS region of the complex might directly regulate electron flow from the quinol or semiquinone in an electrostatic way.

The model predicts correctly the effect of DNP-INT as the result of inhibition of quinol oxidation at the Q_z-site (reaction step 2 in Fig. 8; results not shown). Also the effect of inactivation of plastocyanin by treatment with KCN was correctly simulated with the model. The modified model did not predict that in the presence of DBMIB a transient input of electrons to the oxidizing side of PS I was observed (Fig. 5). Other studies [57,58,59] indicated that the mechanism of inhibition of DBMIB is possible more complicated that just inhibition of the Q_z-site.

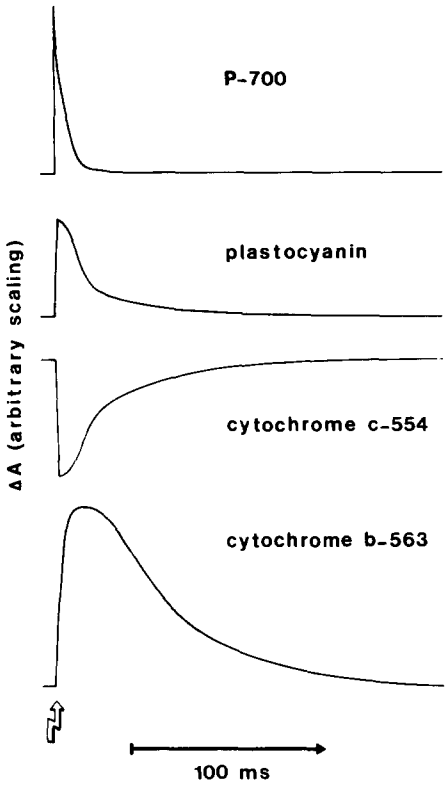

Fig. 9. A computer simulation of the observed flash-induced absorption transients of P-700, plastocyanin, and the cytochromes *c*-554 and *b*-563 at 525, 590, 554 and 563 nm, respectively (cf. Fig. 4). The simulation was according to Fig. 8, with the additional assumptions that: (1) the semiquinone could also oxidize cytochrome *b*-563 and reduce the Rieske FeS centre, and (2) quinol- or semiquinone-dependent reduction of the Rieske FeS centre was proportional to the fifth power of the cytochrome *c*-554 concentration. The stiff differential equations were numerically evaluated according to a 4th-order Runge-Kutta method [56] in steps of 100 μs (same results with 50 μs steps). The evaluation started at full reduction of the components, except cytochrome *b*-563 and P-700, which were fully oxidized. The scaling was identical for each of the four traces shown. Ferredoxin was not taken into account. The open arrow indicates the moment where the evaluation started ('flash').

The site of antimycin inhibition

The mechanism of antimycin inhibition in chloroplasts has been subject to debate [18,20,39,47, 49,57,61–62]. Also from Fig. 5, this mechanism is not immediately apparent. In analogy with its effect in the mitochondrial cytochrome bc complex, antimycin may inhibit reoxidation of cytochrome *b*-563 at the Q_c-site. Indeed, Fig. 5 shows that reoxidation of cytochrome *b*-563 is inhibited. However, also the reduction of the cytochrome is inhibited. To explain this, several possibilities may be considered.

In the first place this effect may be due to insufficient relaxation of the reduction (i.e., insufficient reoxidation) between flashes, leading to an increasingly small extent of the flash-induced cytochrome *b*-563 reduction, and thus to a smaller extent of the averaged signal. (The flash-frequency- and redox-potential-dependent behaviour is still under investigation and will be published later). If, due to insufficient relaxation, cytochrome *b*-563 would indeed stay reduced between the flashes in the presence of antimycin, electron transfer to the Rieske FeS centre and cytochrome *c*-554 would be inhibited, as is indeed observed (Fig. 5). Incidently, this implies that under these conditions, oxidation of the semiquinone at the Q_z-site by Rieske FeS centre (as indicated by our simulations) is slow.

In the second place antimycin may additionally block the Q_z-site. Note that antimycin was present at rather high concentrations [18,47,49,62], although in other studies antimycin was observed to become effective only at concentrations in the range of 10–50 μM [17,20,63]. An inhibitory effect of antimycin at the Q_z-site would also explain the inhibition of the rereduction of cytochrome *c*-554, plastocyanin and P-700.

Both these mechanisms of antimycin inhibition do not readily explain why there is a transient input of electrons from plastoquinol to the oxidizing side of PS I (Fig. 5). Isolated cytochrome *bf* complex is remarkably insensitive to antimycin [60]. Although binding studies showed that high-specific binding sites for antimycin were indeed present in chloroplasts [61,62], they were not found on the cytochrome *bf* complex, but on another thylakoid protein, probably associated with ferredoxin-dependent plastoquinone reduction [61].

A third and probably most likely possibility would be that antimycin did not directly affect the cytochrome *bf* complex, but inhibited (ferredoxin-dependent) quinone reduction. If this were the case, in the 10 s between the flashes the quinone pool would become only slowly and incompletely rereduced in the presence of antimycin. When the amount of reducing equivalents in the quinone

pool would be insufficient to rereduce the sum of flash-oxidized cytochrome *c*-554, plastocyanin and P-700, incomplete rereduction will be observed as in the redox balance in Fig. 5 (right). The development of this effect in the course of flashing cannot be observed in the present experiments, because extensive signal averaging was necessary. It was, however, observed in phosphorylation experiments in which ATP synthesis was directly and continuously monitored in the reaction cuvette. There, the inhibition by antimycin appeared to develop after a lag of several flashes [64]. The simulation model predicts that with a blocked cytochrome *b*-563 oxidation and with fully prereduced cytochrome *b*-563, it is still possible to reduce the high-potential components on the oxidizing side of the photosystem completely. That this does not occur is also explained by antimycin inhibition of electron transfer from ferredoxin to the plastoquinone pool.

It should be realized that an antimycin binding-site elsewhere than on the cytochrome *bf* complex does not imply that a Q_c-site (where cytochrome *b*-563 is oxidized by a semiquinone) does not exist, nor does it imply that oxidation of cytochrome *b*-563 should not be (indirectly) inhibited by antimycin. Our results are best explained by assuming the existence of an antimycin-sensitive component in the electron pathway from ferredoxin to the quinone pool, but this pathway may involve ('reductant-induced') oxidation of cytochrome *b*-563 (see below).

Electron transfer from ferredoxin to the quinone pool

A question of interest is whether oxidation of ferredoxin yields plastoquinol, or perhaps a semiquinone radical (as in the mechanism proposed by Chain [42] to explain reductant-induced oxidation). Because it is not possible to block flash-induced reduction of cytochrome *b*-563 by imposing very reduced conditions on the ferredoxin (as in the experiment in the presence of dithionite), we conclude that cytochrome *b*-563 does not equilibrate with the ferredoxin or plastoquinone/plastoquinol redox potential. This implies that, under 'normal' conditions, cytochrome *b*-563 at a given site equilibrates only with a single step in the two-step redox couple quinone/quinol.

As a result of our method of redox-poising (with NADPH and oxygen via ferredoxin) we cannot evaluate reductant-induced oxidation of cytochrome *b*-563 (as in the proposal by Chain [42]) on the basis of the discrepancy between the apparent kinetics of reoxidation of cytochrome *b*-563 and ferredoxin. After each flash, there is a redistribution of electrons between the (reduced) ferredoxin, the (oxidized) quinone pool, the ferredoxin-NADPH oxidoreductase and the $NADP^+$/NADPH couple, but the redox changes of the latter two components were not resolved in these experiments.

Acknowledgements

This work was supported in part by the Foundations for Biophysics and for Chemical Research (SON), with financial support from the Netherlands Foundation for Scientific Research (NWO). The expert technical assistance of C. Wattel, D. van Marum and the late J.H. van Leeuwen is gratefully acknowledged. The authors thank F. van Mourik for suggesting the deconvolution method, and F.J. Leeuwerik for partial adaptation of the deconvolution computer program.

References

1 Peters, A.L.J., Van Wielink, J.E., Wong Fong Sang,H.W., De Vries, S. and Kraayenhof, R. (1983) Biochim. Biophys. Acta 724, 159–165.
2 Peters, A.L.J., Van der Pal, R.H.M., Peters, R.L.A., Vredenberg, W.J. and Kraayenhof, R. (1984) Biochim. Biophys. Acta 766, 169–178.
3 Peters, A.L.J., Smit, G.A.B., van Diepen, A.T.M., Krab, K. and Kraayenhof, R. (1984) Biochim. Biophys. Acta 766, 179–187.
4 De Wolf, F.A., Groen, B.H., Van Houte, L.P.A., Peters, A.L.J., Krab, K. and Kraayenhof, R. (1985) Biochim. Biophys. Acta 809, 204–214.
5 Kraayenhof, R., de Wolf, F.A., Van Walraven, H.S. and Krab, K. (1986) Bioelectrochem. Bioenerg. 16 (J. Electroanal. Chem 212), 273–285.
6 Peters, A.L.J., Van Spanning, R. and Kraayenhof, R. (1983) Biochim. Biophys. Acta 724, 159–165.
7 De Wolf, F.A., Galmiche, J.M., Kraayenhof, R. and Girault, G. (1985) FEBS Lett. 192, 271–274.
8 De Wolf, F.A., Galmiche, J.M., Krab, K., Kraayenhof, R. and Girault, G. (1986) Biochim. Biophys. Acta 851, 295–312.
9 Bouges-Bocquet, B. (1981) Biochim. Biophys. Acta 635, 327–340.

10 Houchins, J.P. and Hind, G. (1983) Biochim. Biophys. Acta 725, 138–145.
11 Lam, E. (1984) FEBS Lett. 172, 255–260.
12 Girvin, M.E. and Cramer, W.A. (1984) Biochim. Biophys Acta 767, 29–38.
13 Jones, R.W. and Whitmarsh, J. (1985) Photobiochem. Photobiophys. 9, 119–127.
14 Van Kooten, O., Gloudemans, A.G.M. and Vredenberg, W.J. (1983) Photobiochim. Photobiophys. 6, 9–14.
15 Joliot, P. and Joliot, A. (1984) Biochim. Biophys. Acta 765, 210–218.
16 Rich, P.R., Heathcote, P. and Moss, D.A. (1987) Biochim. Biophys. Acta 892, 138–151.
17 Garab, G., and Farineau, J. (1983) Biochem. Biophys. Res. Commun. 111, 619–623.
18 Moss, D.A. and Bendall, D.S. (1984) Biochim. Biophys. Acta 767, 389–395.
19 Giorgi, L.B., Packham, N. and Barber, J. (1985) Biochim. Biophys. Acta 806, 366–372.
20 Barabas, K., Zimányi, L. and Garab, G. (1985) J. Bioenerg. Biomembr. 17, 349–364.
21 Moss, D.A. and Bendall, D.S. (1986) Biochem. Soc. Trans. (Lond.) 14, 57–58.
22 Hiyama, T. and Ke, B. (1972) Biochim. Biophys. Acta 267, 160–171.
23 Tagawa, K, and Arnon, D.I. (1962) Nature 195, 537–541.
24 Katoh, S., Shiratori, I. and Takamiya, A. (1962) J. Biochem. 51, 32–40.
25 Wasserman, A.R. (1980) Methods Enzymol. 69, 181–202.
26 Venturoli, G. Virgili, M., Melandri, B.A. and Crofts, A.R. (1987) FEBS Lett. 219, 477–484.
27 Berry, E.A. and Trumpower, B.L. (1987) Anal. Biochem. 161, 1–15.
28 Schuurmans, J.J., Leeuwerik, F.J., Oen, B.S. and Kraayenhof, R. (1981) in: Photosynthesis, Vol. 1 (Akoyunoglou, G., ed.), pp. 543–552, Balaban International Science Services, Philadelphia, PA.
29 Kraayenhof, R. Schuurmans, J.J., Valkier, L.J., Veen, J.P.C., Van Marum, D. and Jasper, C.G.G. (1982) Anal. Biochem. 127, 93–99.
30 Shin, M. and Arnon, D.I. (1965) J. Biol. Chem. 240, 1405–1411.
31 Foust, G.P., Mayhew, S.G. and Massey, V. (1969) J. Biol. Chem. 244, 964–970.
32 Bhattacharyya, A.K., Meyer, T.E. and Tollin, G. (1986) Biochemistry 25, 4655–4661.
33 Cramer, W.A. and Whitmarsh, J. (1977) Annu. Rev. Plant Physiol. 28, 133–172.
34 Strang, G. (1980) Linear Algebra and its Applications, pp. 1–45, Academic Press, Orlando, FL.
35 Sétif, P. and Mathis, P. (1986) in: Encyclopedia of Plant Physiology, Vol. 19 (Staehelin, A. and Arntzen, C.J., eds.), pp. 477–479, Springer, Berlin.
36 Izawa, S. Kraayenhof, R., Ruuge, E.K. and De Vault, D. (1973) Biochim. Biophys. Acta 314, 328–339.
37 Haehnel, W. (1977) Biochim. Biophys. Acta 459, 418–441.
38 Bendall, D.S. (1982) Biochim. Biophys. Acta 683, 119–151.
39 Mills, J.D., Crowther, D., Slovacek, R.E. and Hind, G. (1979) Biochim. Biophys. Acta 547, 127–137.
40 Cox, R.P. (1979) Biochem. J. 184, 39–44.
41 Lam, E. and Malkin, R. (1982) FEBS Lett. 141, 98–101.
42 Chain, R.K. (1982) FEBS Lett. 143, 273–278.
43 Hauska, G., Hurt, E., Gabellini, N. and Lockau, W. (1983) Biochim. Biophys. Acta 726, 97–133.
44 Rich, P.R. (1984) Biochim. Biophys. Acta 768, 53–79.
45 Rich, P.R. (1985) Photosynth. Res. 6, 335–348.
46 Bergström, J., Andréasson, L.E. and Vänngård, T. (1986) Biochim. Biophys. Acta 852, 112–118.
47 Hartung, A. and Trebst, A. (1985) Physiol. Vég. 23, 635–648.
48 Malkin, R. (1986) FEBS Lett. 208, 317–320.
49 Slovacek, R.E., Crowther, D. and Hind, G. (1979) Biochim. Biophys. Acta 547, 138–148.
50 Crofts, A.R. and Wraight, C.A. (1983) Biochim. Biophys. Acta 726, 149–185.
51 Moss, D.A. and Rich,P.R. (1987) Biochim. Biophys. Acta 894, 189–197.
52 Rich, P.R. and Wikström, M. (1986) FEBS Lett. 194, 176–182.
53 Wikström, M. and Krab. K. (1986) J. Bioenerg. Biomembr. 18, 181–193.
54 Joliot, P. and Joliot, A. (1986) Biochim. Biophys. Acta 849, 211–222.
55 Delosme, R., Joliot, P. and Trebst, A. (1987) Biochim. Biophys. Acta 893, 1–6.
56 Pennington, R.H. (1970) Introductory Computer Methods and Numerical Analysis, pp. 457–493, MacMillan, London.
57 Willms, I., Malkin, R. and Chain, R.K. (1987) Arch. Biochem. Biophys. 258, 248–258.
58 Degli Esposti, M., Rotillo, G. and Lénaz, G. (1984) Biochim. Biophys. Acta 767, 10–20.
59 Rich, P.R. and Bendall, D.S. (1981) in: Vectorial Reactions in Electron and Ion Transport in Mitochondria and Bacteria (Palmieri, F., Quagliariello, E., Siliprandi, N. and Slater, E.C., eds.), pp. 187–190, Elsevier/North-Holland Biomedical Press, Amsterdam.
60 Hurt, E. and Hauska, G. (1981) Eur. J. Biochem. 117, 591–599.
61 Davies, E.C. and Bendall, D.S. (1987) in: Progress in Photosynthesis Research (Biggins, J., ed.), Vol. II, pp. 485–488, Martinus Nijhoff, Dordrecht.
62 Mills, J.D., Slovacek, R.E. and Hind, G. (1978) Biochim. Biophys. Acta 504, 298–309.
63 Shahak, Y., Crowther, D. and Hind, G. (1981) Biochim. Biophys. Acta 636, 234–243.
64 De Wolf, F.A., Galmiche, J.M. and Kraayenhof, R. (1988) FEBS Lett, 235, 278–282.